Neurochem Res (2014) 39:950–960
DOI 10.1007/s11064-014-1292-4

ORIGINAL PAPER

Hyperbaric Oxygen Therapy Ameliorates Local Brain Metabolism, Brain Edema and Inflammatory Response in a Blast-Induced Traumatic Brain Injury Model in Rabbits

Yongming Zhang · Yanyan Yang · Hong Tang · Wenjiang Sun · Xiaoxing Xiong · Daniel Smerin · Jiachuan Liu

Received: 18 November 2013 / Revised: 13 March 2014 / Accepted: 20 March 2014 / Published online: 30 March 2014

Abstract Many studies suggest that hyperbaric oxygen therapy (HBOT) can provide some clinically curative effects on blast-induced traumatic brain injury (bTBI). The specific mechanism by which this occurs still remains unknown, and no standardized time or course of hyperbaric oxygen treatment is currently used. In this study, bTBI was produced by paper detonators equivalent to 600 mg of TNT exploding at 6.5 cm vertical to the rabbit's head. HBO (100 % O_2 at 2.0 absolute atmospheres) was used once, 12 h after injury. Magnetic resonance spectroscopy was performed to investigate the impact of HBOT on the metabolism of local injured nerves in brain tissue. We also examined blood–brain barrier (BBB) integrity, brain water content, apoptotic factors, and some inflammatory mediators. Our results demonstrate that hyperbaric oxygen could confer neuroprotection and improve prognosis after explosive injury by promoting the metabolism of local neurons, inhibiting brain edema, protecting BBB integrity, decreasing cell apoptosis, and inhibiting the inflammatory response. Furthermore, timely intervention within 1 week after injury might be more conducive to improving the prognosis of patients with bTBI.

Keywords Brain injury · Explosive injury · Rabbit · Magnetic resonance spectrum · Hyperbaric oxygen

Y. Zhang (✉) · Y. Yang · H. Tang · W. Sun · J. Liu (✉)
Department of Neurosurgery, No. 105 Hospital of PLA, Anhui Medicine University, Hefei 230031, People's Republic of China
e-mail: zymhf2966@163.com

J. Liu
e-mail: zym_105sjw@163.com

Y. Zhang · X. Xiong
Department of Neurosurgery, Stanford University, Stanford, CA 94306, USA

D. Smerin
School of Medicine, Stanford University, Stanford, CA 94306, USA

Introduction

Blast-induced traumatic brain injury (bTBI), with severe trauma and poor prognosis, is an important cause of severe craniocerebral injury in wars or peacetime and can result in death and disability [1–4]. A large number of retrospective studies suggest that hyperbaric oxygen therapy (HBOT) can provide some clinically curative effects on brain injury, including improving the prognosis of patients and shortening the duration of coma. But the specific mechanism underlying these observations still remains unknown, and no standardized time or course of hyperbaric oxygen treatment currently exists [5–9]. MRS can be used to non-invasively detect energy metabolism and biochemical changes of tissues and organs in vivo, as well as carry out quantitative analysis of compounds. MRS can also be used to further investigate the metabolism of diseases based on magnetic resonance imaging (MRI) morphology [10, 11]. In this study, MRS was performed on rabbits with blast-induced brain injury before and after HBOT. The impacts of HBOT on the metabolism of local injured nerves in brain tissue were then investigated and analyzed in order to provide scientific clues and a basis for the selection of a regimen for HBOT. Furthermore, to study the mechanism of HBOT on bTBI, we examined blood–brain barrier (BBB) integrity, brain water content, apoptotic factors, and some inflammatory mediators.

Materials and Methods

Experimental Animals

Healthy adult New Zealand white rabbits, male, weighing 2.0–2.5 kg, were provided by the Experimental Animal Center, Research Institute of Field Surgery, Daping Hospital, Third Military Medical University, Chongqing, China. They were randomly divided into a bTBI, HBOT, and sham group. All of the experimental protocols were approved by the local animal experimentation and ethics committee.

Establishment of Explosive Brain Injury Models

Explosive brain injury models were created with rabbits using paper detonator exploding methods described previously [12, 13]. All rabbits were fed for 7 days before experimentation, and were anesthetized by intravenous injection of 3 % pentobarbital sodium (1 mg/kg) via the auricular vein. After shaving, Electrocardiograph electrodes were placed in the precordial region, while an arterial line was inserted into the right femoral artery and connected to a multi-functional physiological monitor. Then, the rabbit was placed in the prone position in a specially wooden box, with only its head protruding outside through an opening. A TNT equivalent paper detonator (600 mg, 6.0 mm diameter and 3.0 cm length, 845 Factory, Chongqing, China), which was connected with a detonating cord and detonated by dry batteries, was detonated above the rabbit's head at the following coordinates: 6.5 cm vertical from scalp, 1.5 cm lateral from sagittal suture and 2 cm anterior from binaural line. The pressure of the explosion was detected by the Wavebook/516A Pressure Test System (Quatronix Inc. Akron, OH, USA). Debridement and suturing were performed after the explosion. The sham group was only subjected to incision and suturing of the focal skin.

Respiration rate and rhythm, along with heart rate were carefully observed in each group. Cardiopulmonary resuscitation was immediately performed if a respiratory pause occurred. Apnea time, recovery time, heart disorders, and mean arterial pressure after injury were also recorded. A left femoral artery was catheterized for monitoring continuous blood pressure and sampling periodic blood for arterial gases and pH (Rapidlab 1200 analyzer, Bayer AG, Leverkusen, Germany) at 30 min before the explosion and 24 h after the explosion. Blood glucose levels were assayed simultaneously using a Glucose Monitor (Glucose Lifescan OneTouch SureStep Blood Glucose Monitor, JNJ, USA).

Hyperbaric Oxygen Treatment Plan

A hyperbaric oxygen chamber (transparent hyperbaric pure oxygen chamber) was purchased from Shanghai Regulator Company, China. After successful establishment of the animal model and presence of stable vital signs, every rabbit in the HBOT subgroup was treated once with different courses of hyperbaric oxygen treatment 12 h after trauma with 2 absolute atmosphere (ATA) pressure 100 % O_2, boosting pressure for 30 min, stable pressure for 1 h, and reducing pressure for 30 min. Rabbits in the other groups were only supplied air at normal pressure.

MRI Plain Scan and MRS Examinations

MRI plain scan and MRS examinations were performed at different time points following trauma in the bTBI group and following treatment in the HBOT group. A small joint coil was placed in the middle of the bedstead, and the coil was adjusted toward the magnetic field center as much as possible. The rabbits were in the prone position. The head of the rabbit was placed in the center of the coin, and the body of the rabbit was covered with cotton sheets in order to avoid death by an anesthetized low-temperature state. The following procedures have been previously described [14–16]. Briefly (1) MRI scans: axial, sagittal, coronal SE T_1WI positioning images were scanned, followed by axial fast spin-echo sequence T_2WI, with 2,500 ms TR, 135 ms TE, 3 mm slice thickness and no spacing for 9 layers, FOV19, NEX2. Thus, six layers of satisfying axial images were usually obtained. (2) MRS scans: the central largest layer was selected for axial T_2WI to avoid influence from the cranial wall and base of skull. Single voxel MRS was performed in sites with obvious cerebral contusion and corresponding lateral sites in T_2 phase. The voxel size was $5.1 \times 5.1 \times 5.0$ mm. Pressurized water suppression scans with point-resolved spectroscopy were then performed eight times, and motivations were performed 128 times. The scanning in the remaining areas was performed by automatic pre-scanning procedures. The resolution of FWHMZ was less than 0.1 ppm, with a water inhibition level of 99 %. (3) Parameter analysis: three peaks of metabolins including NAA, Cho and Cr in proton spectroscopy were automatically recognized by software, and the area under the curve of each metabolin was automatically calculated. Then, the NAA/Cr ratio, Cho/Cr ratio, and NAA value were calculated according to the signal strength of each metabolin.

Pathological Examination and Measurement of Brain Contusion Volume

Rabbits ($n = 10$ in each group) were sacrificed with intravenous injection of air (20 ml) via auricular vein at different time points. The rabbits were then placed in the

supine position. The thoracic cavity was cut open to expose the heart, and the right atrial appendage was cut open after the left ventricle was intubated. Heart chambers were rapidly perfused with 200 ml normal saline until outflow liquid was clear and bright. The heart was then perfused with 200 ml 0.1 M PBS (pH 7.3) containing 4 % paraformaldehyde. Brain tissue was then harvested for HE staining and brain contusion measurement. Brain slices with the biggest contusion areas were photographed in order to determine the contusion proportion of the whole brain after a series of 5 mm-thick slices were created. Histopathological indices of center brain contusion and penumbra were recorded using an optical microscope. Image J software was used to calculate the relative area of the central contusion and penumbra (a percentage of the contralateral hemisphere).

Edema Measurement by Wet–Dry Weight Methods

Brain tissue from traumatic and contralateral hemispheres in two groups of rabbits (n = 3 at each time point) were harvested. Blood clots on the surface of brain were removed with filter paper. Brain tissue was then placed on weighed aluminum foil, and the wet weight was determined using an electronic balance with a precision of up to one thousandth of a gram. Subsequently, the brain tissues were placed in a constant temperature drying oven at 110 °C for 24 h and then weighed again for dry weight. Water content (%) was calculated according to the following formula: water content of brain tissues (%) = (wet weight−dry weight)/wet weight × 100 %.

Evaluation of BBB Integrity

To examine whether HBOT prevents BBB leakage, BBB integrity in the experimental animals (n = 3 at each time point) was studied using Evans blue (EB) [17, 18]. The time course of BBB leakage in bTBI rabbits was studied at 1, 6, 12, 24, 48 and 72 h after injury. Since HBOT was conducted once 12 h after injury, the effect of HBOT on BBB was examined at 24 and 48 h after injury. EB (4 %, 2 ml/kg) was injected intravenously into rabbits, and the rabbits were perfused with heparinized saline solution 2 h later. Brain tissue was harvested and the contusion core, injury ipsilateral rest hemisphere, and contralateral cortex were dissected, weighed, homogenized, and incubated in 500 ml formamide at 54 °C for 2 h. The solution was centrifuged at 12,000*g* for 15 min, and the supernatant removed. EB was measured using spectrophotometry (absorbance at 620 nm; Spectro Max 340, Molecular Devices, Sunnyvale, CA, USA). The amount of EB was computed based on external standards in the same solvent (1–20 mg/ml) and expressed as per gram of tissue.

Reverse Transcription Polymerase Chain Reaction (RT-PCR)

To verify that HBOT can exert the effect of neuronal protection in brain injury, we detected caspase-3 at 1 and 3 day after injury in both the bTBI and HBOT groups (n = 3 in each subgroup). We further studied some inflammatory parameters such as IL-8 and TNF-α levels at 6, 12, 24, and 48 h after injury. RNA extraction and RT-PCR for IL-8 and TNF-α, the animals (n = 3 at each time point) were sacrificed with 20 ml via intravenous injection of air into the auricular vein and their brains were removed. Brain tissue surrounding the injury site was harvested (0.5 cm from the margin of injury, approximately 3.0 mm^3). Total RNA was extracted using TRIzol reagent (Invitrogen, USA) according to the manufacturer's instructions. The RNA yield and purity were assessed by spectrophotometric analysis. Total RNA (500 ng) from each sample was subjected to reverse transcription with random nonamer, dNTP and AMV reverse transcriptase in a 10 μl reaction mixture. The PCR of cDNA was carried out using Takara Ex Taq Hotstart polymerase, dNTPs and the following related primers: 5′GG AGCTGGACTGTGGCATTGA (sense) and 3′AGGTACG AGTGCTTTCTTGAC (antisense) for caspase-3, 5′TGTGG GTCTGTTGTAGGG (sense) and 3′CGGTGGTAGAAT GGAGTG (antisense) for IL-8; 5′CACGCTCTTCTGTC TACTGAG (sense) and 3′GGACTCCGTGATGTCTAAGT (antisense) for TNF-α; 5′ATTGTTGCCATCAACGACC (sense) and 3′CGAGTACTGGTGTCAGGTAC (antisense) for GAPDH. After denaturation for 3 min at 94 °C, the total amount of reaction products was amplified for 30 cycles (94 °C, 30 s; 58 °C, 30 s; 72 °C, 120 s) on the TAKARA PCR Thermal Cycler. PCR products were separated by electrophoresis through 1.2 % agarose containing 0.5 μg/ml ethidium bromide and imaged using a BioDoc-IT imaging system (Bio-Rad, Hercules, CA, USA). Band intensities were determined using GS-710 calibrated imaging Densitometer (Bio-Rad). All signals were standardized against the GAPDH mRNA signal for each sample and the results are expressed as a percentage of the expression of GAPDH.

Western Blot Analysis

To quantify the expression of caspase-3, IL-8 and TNF-α, we further performed western blotting. Brain tissue surrounding the injury site (0.5 cm from the margin of injury, approximately 3.0 mm^3) was harvested, as described above. The tissue was sonicated in lysis buffer to extract and determine total protein. Each sample was electrophoresed on 10 % sodium dodecyl sulfate polyacrylamide gel electrophoresis and then transferred to nitrocellulose membranes. Membranes were blocked in 5 % non-fat milk in 50 mM Tris-buffered saline (pH 7.4) containing 0.1 %

Tween-20 (TBS-T) for 1 h at room temperature, washed in TBS-T and incubated overnight with rabbit polyclonal antibody to caspase-3; IL-8 and TNF-α (Santa Cruz Biotechnology; Santa Cruz, CA, USA) at dilutions of 1:1,000, 1:500 and 1:1,000. On the second day the membranes were washed and further incubated in blocking solution with peroxidase-conjugated goat anti-rabbit antibody (Santa Cruz Biotechnology, Santa Cruz, CA, USA) for 1 h at room temperature. In all immunoblotting experiments, the blots were reprobed with an antibody against β-actin (1:3,000; Sigma-Aldrich), which were used as protein loading controls. Membranes were scanned using Typhoon Trio (GE Healthcare). Optical densities of all protein bands were analyzed using Imagequant 5.2 software (GE Healthcare).

Statistical Analyses

All data were collected and analyzed in a blind fashion and have shown normal distribution. Data were expressed as the mean ± SEM and analyzed for statistical significance using one-way analysis of variance followed by Scheffe's test for multiple comparisons. Statistical differences were considered significant at $p < 0.05$ or $p < 0.01$.

Results

Animal Modeling and Physiological Parameters

One hundred forty-six New Zealand white rabbits were subjected to brain explosive injury, contributing to the successful establishment of an explosive injury animal model. The pressure of an explosion created by a 600 mg TNT equivalent paper detonator at 6.5 cm vertical distance was 638.2 ± 23.9 kPa. The rise time and duration of the positive pressure was 0.1 and 0.18 ms, respectively, with an impulse of 59.42 Pa.

All rabbits were woken at 1–2 h after explosion. Most rabbits were apathetic and exhibited poor appetite after awakening. Internal organ damage, especially lung injury, were not found owing to the protective wooden box. Three rabbits died from intracranial hematoma, 2 died from intracranial infection, 1 died 4 days later from poor food intake, 3 suffered from epilepsy and paralysis of the limbs, and the remaining rabbits survived for at least 7 days. The mean apnea time was 67.02 ± 9.08 s, heart rate decreased by 30.16 ± 3.07 times/min, and arterial blood pressure increased by 39.41 ± 9.38 mmHg. Temporal apnea was instantaneously observed after the explosion, followed by deeper and slower breathing. Breathing then gradually accelerated, while blood pressure increased and heart rate decreased. Other physiological variables, summarized in Table 1, including mean arterial blood pressure, blood gases, blood pH and serum glucose, were not significantly different between groups at both 30 min before and 24 h after the explosion.

HBOT reduces the penumbra size around the contusion region and inhibits neuronal edema and inflammatory cell infiltration.

Anatomical physiology showed that the focal cerebral lacerated wound was mainly located in the posterior parietal cortex (Fig. 1a, b). In the bTBI group, observation under a microscope showed that continuous fracture, bleeding, and contusion alteration appeared in the cerebral cortex. Neurons exhibited swelling, degeneration and necrosis. Cell nuclei structure was not clear, and some exhibited pyknosis. A large number of inflammatory cells gathered in the capillaries and infiltrated into the injury region (Fig. 1e). These characteristic pathological changes in neurons and inflammatory cells were significantly lessened in the HBOT brains (Fig. 1f). Additionally, one tissue

Table 1 Physiological parameters

	pH	pO_2	pCO_2	MABP	Glucose
30 min before explosive injury					
bTBI	7.35 ± 0.31	190.09 ± 10.02	34.10 ± 3.90	72.10 ± 3.24	5.35 ± 0.15
HBOT	7.36 ± 0.19	189.10 ± 6.13	35.25 ± 5.65	73.21 ± 5.31	5.75 ± 0.25
Sham	7.35 ± 0.57	190.21 ± 17.25	34.17 ± 3.07	72.00 ± 3.98	5.49 ± 1.31
24 h after explosive injury					
bTBI	7.33 ± 0.39	187.30 ± 13.29	37.81 ± 3.98	84.21 ± 3.08*	10.49 ± 0.47*
HBOT	7.35 ± 0.27	210.51 ± 11.31*	32.59 ± 6.54	73.76 ± 4.61	8.31 ± 2.09
Sham	7.35 ± 0.59	189.73 ± 8.47	34.71 ± 3.15	75.41 ± 10.09	5.36 ± 0.43

A left femoral artery was catheterized for monitoring continuous blood pressure and sampling periodic blood for arterial gases and pH

pH power of hydrogen, *MABP* mean arterial blood pressure, pO_2 partial pressure of oxygen, pCO_2 partial pressure of carbon dioxide

* Significant difference compared with sham group ($p < 0.05$)

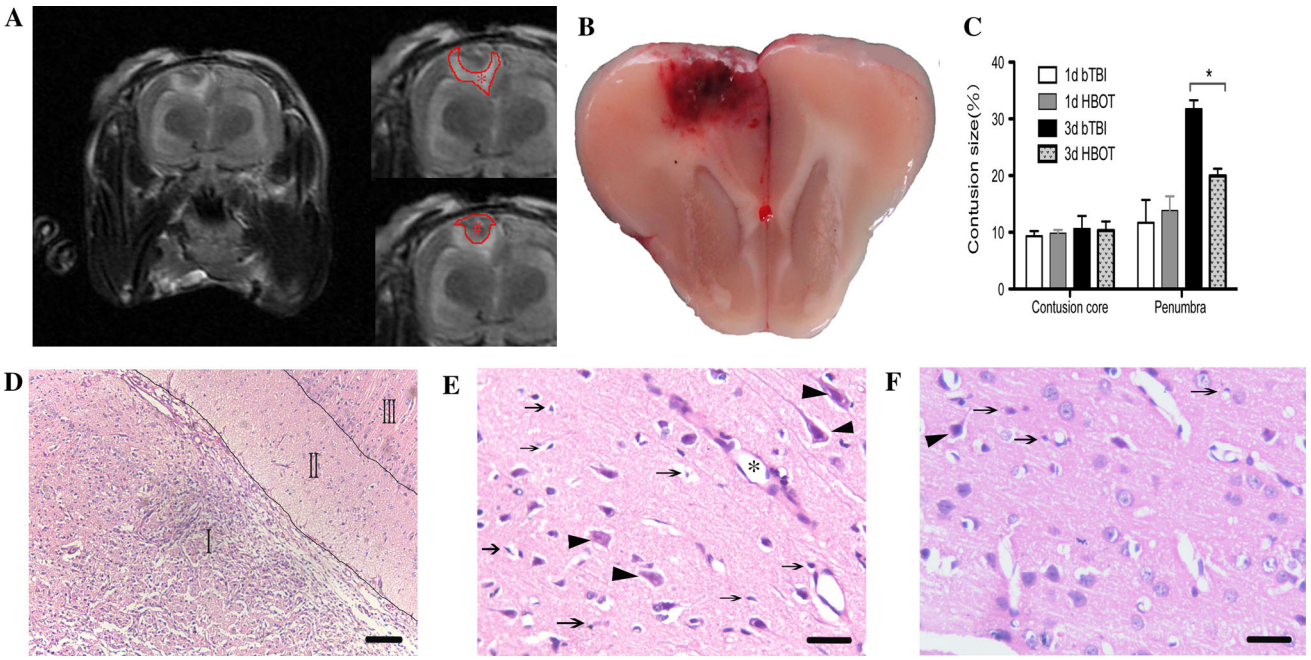

Fig. 1 HBOT reduces the penumbra size around the contusion region and inhibits neuronal edema and inflammatory cell infiltration. **a** MRI image of blasted traumatic brain in T2WI. *Asterisk* penumbra and *hash* contusion core. **b** Coronal section profile of rabbit brain subjected to bTBI. **c** The size of contusion and penumbra changes with/without HBOT treatment. *Significant difference ($p < 0.05$). **d** HE staining picture of blast brain tissue (×100). Area *I*, *II*, *III*, indicates respectively contusion core region, penumbra, and normal brain tissue. *Bar* 100 μm. **e** HE staining picture of brain tissue 3 days after injury in the bTBI shows swollen neurons (*arrow head*), nuclear fragmentation and pyknosis (*arrow*), and accumulating inflammatory cells (*astreiks*) within the brain microvasculature (×400). *Bar* 25 μm. **f** Image of brain tissue 3 days after injury in HBOT shows much less swelling in neurons, nuclear fragmentation and pyknosis (×400). *Bar* 25 μm

environment was observed between brain contusion core and normal brain tissue, which exhibited some distinguished characteristics with slight dyeing, enlargement and edema of interstitial space, but normal structure and shape of most neurons and microglia (Fig. 1d). Based on these properties, the region was recognized as the ischemic penumbra, which was outlined clearly and easily in the MRI (Fig. 1a). Compared with the ratio of the bTBI group, the ratio of the ischemic penumbra region size to the contralateral hemisphere size was lower in the HBOT group ($p < 0.05$) at 1 and 3 days after brain damage. However, the ratio of the contusion core size to the contralateral hemisphere size did not show significant alteration between the two groups (Fig. 1c).

HBOT Ameliorates Local Brain Metabolism in Blast Injury Rabbits

MRS examination was performed at varying time points, with results being listed in Fig. 2. NAA/Cr value in the bTBI group immediately declined after injury, followed by a rebound from 24 h after injury, and declined again 7 days later. By contrast, the rebound NAA/Cr level in the HBOT group was earlier than the bTBI group, and the value at different time points significantly increased, especially within 1 week after brain injury ($p < 0.01$). Cho/Cr value elevated after injury, and then declined 12 h later, but gradually rebounded 3 days later. The difference in Cho/Cr value between the HBOT and bTBI groups was significant, particularly at 24 h and 3 days after injury ($p < 0.05$).

HBOT Decreases Water Content in Blast Brain Tissue

The water content of rabbit cerebral cortex tissue after trauma first increased and was then gradually restored (Fig. 3). Water content started to increase 1 h after trauma, and continued to gradually increase at 6, 12, and 24 h. Water content peaked at 72 h, and then gradually decreased. Interestingly, the water content of cerebral cortex tissue in the HBOT group was significantly less than that of the trauma group at each time point, particularly at 12–72 h after injury ($p < 0.01$). Water content was nearly restored to normal amounts 14 days after injury.

HBOT Suppresses BBB Permeability Induced by Explosive Injury

BBB permeability was measured using EB. The content of EB in brain tissue increased as early as 6 h, remained

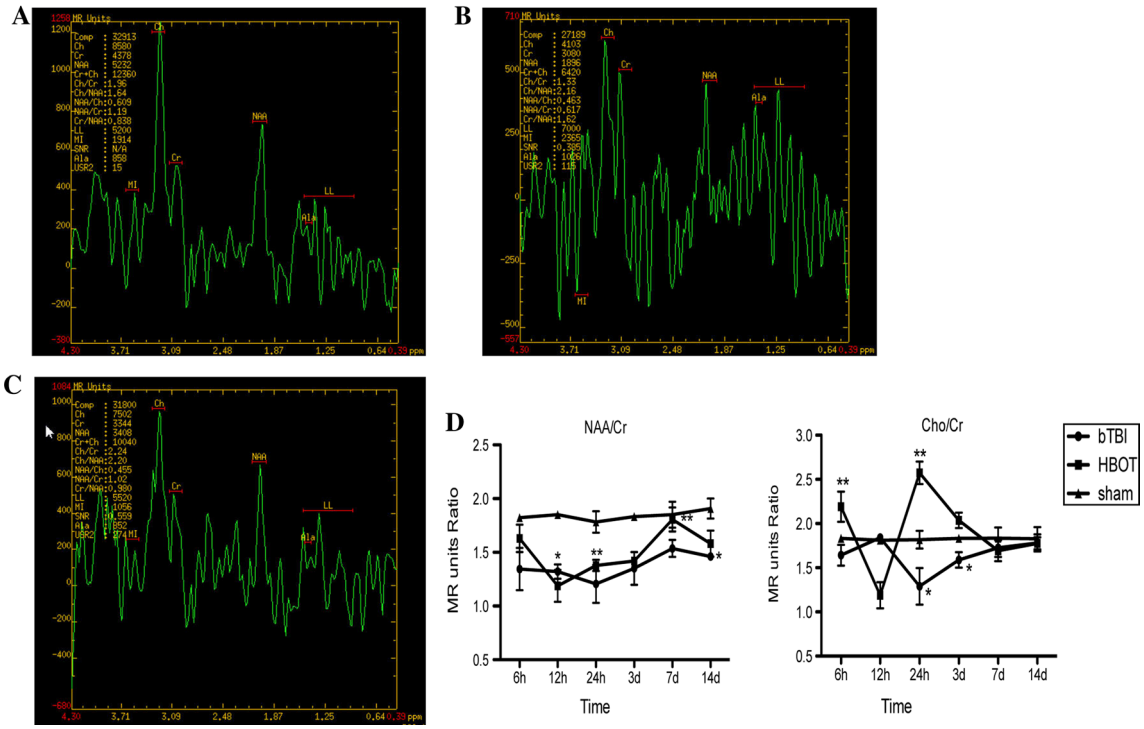

Fig. 2 HBOT ameliorates local brain metabolism according to the results of MRS in blast injury rabbits. **a** Typical spectrum in the sham group. **b** Typical spectrum in the brain injury group (3 days post-injury). **c** Typical spectrum in the treatment group (3 days post-injury). **d** The mean NAA/Cr and Cho/Cr changes at different time points in the bTBI, HBOT and sham groups. *Significant difference compared with the control group ($p < 0.05$); **significant difference compared with the model group ($p < 0.01$)

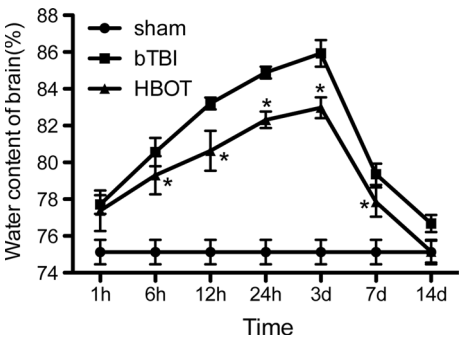

Fig. 3 HBOT decreases water content in blast brain tissue, particularly at 12–72 h after injury. *Significant difference compared with the control group ($p < 0.05$); **significant difference compared with the model group ($p < 0.01$)

unchanged at 1 h, but robustly increased at 48 h after the explosion in the injury hemisphere, suggesting a time-dependent BBB leakage. However, BBB leakage reached a peak at 6 h in the contusion core, and further increases in BBB leakage were not detected at 24 and 48 h. Much higher content of EB was detected in the core than in the penumbra. Compared with the bTBI group, the HBOT group had a significant decline in EB staining at 24 and 48 h in the injury ipsilateral hemisphere (Fig. 4).

HBOT Inhibits the Expression of Caspase-3, IL-8 and TNF-α RNA

The RNA level of caspase-3 in the HBOT group was significantly lower than that in the bTBI group at the third day after injury ($p < 0.05$; Fig. 5a, b). In the bTBI group, the IL-8 level increased 6 h after injury, and reached its highest at 12 h after injury; thereafter it gradually decreased. The IL-8 level in the HBOT group was low compared with the level in the bTBI group at the same time point, especially at 12 h after injury ($p < 0.05$; Fig. 5d). By contrast, the TNF-α level increased in the bTBI group 6 h after injury, gradually increased until 18 h, and then decreased somewhat after 24 h. However, compared with the corresponding control group, the TNF-α level was significantly lower in the HBOT group at 12 and 24 h after injury ($p < 0.05$; Fig. 5e).

HBOT Reduces the Protein Levels of Caspase-3, IL-8 and TNF-α After Injury

The values of caspase-3 protein followed a similar trend as seen with RT-PCR (Fig. 6a, c). IL-8 protein level, which increased gradually after injury and reached a peak at 12 h, showed statistically significant decreases in the HBOT group compared with the bTBI group at 12 and 24 h after

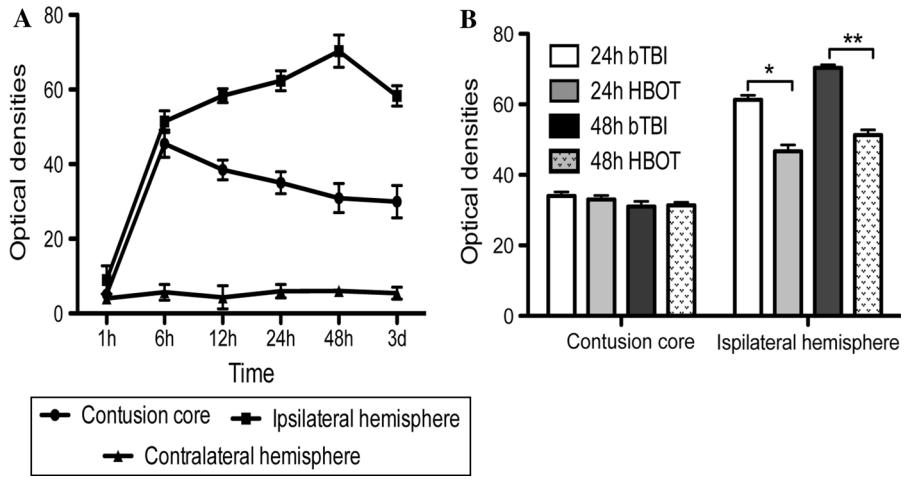

Fig. 4 HBOT suppresses BBB permeability induced by explosive injury. **a** The content of Evan's Blue (EB) increased gradually as early as 6 h after injury and remained unchanged at 1 h. Maximum EB infiltration occurred at 48 h after explosive injury in the injured hemisphere, and reached a peak at 6 h in the contusion core. **b** The HBOT group displayed a significant decline in EB staining at 24 and 48 h in the injury ipsilateral hemisphere. *Significant difference compared with the control group ($p < 0.05$); **significant difference compared with the model group ($p < 0.01$)

injury ($p < 0.05$; Fig. 6e). Additionally, TNF-α level also gradually increased after injury until 18 h, and then decreased. The protein values were much lower in HBOT compared with bTBI at the same time point, with a significant difference occurring at 12 h after injury ($p < 0.05$; Fig. 6d).

Discussion

Explosive bTBI has likely existed since the introduction of gunpowder to warfare. Evidence, mainly from clinical experience, suggests that TBI from explosive blasts is distinct from either closed head TBI (cTBI) or penetrating TBI [1, 3, 19]. Neuroimaging is mainly characterized by skull fracture, brain edema, intracranial hemorrhage and parenchymal contusion. Brain tissue induced by bTBI can develop malignant cerebral edema very quickly, in the order of an hour or so, which is the equivalent of several hours to a day following cTBI [20]. Additionally, cerebral vasospasm was observed in almost 50 % of severe bTBI and even lasted as long as 30 days after injury [20, 21]. HBOT has been used for over 100 years to increase oxygen intake in damaged or oxygen-starved tissues. Evidence of the benefits of HBOT in the treatment of brain injury has been accumulating for the last 30 years with encouraging results [4, 22–24]. Much clinical and animal research supports the idea that patients with mild-to-moderate brain injury can greatly accelerate their recovery and reverse damage with HBOT [25–29]. Despite this supportive evidence, research surrounding HBOT treatment for bTBI has not reported much information, including no standardized time or course of treatment. No specific mechanisms of action for HBOT treatment are known.

In this study, a bTBI model in rabbit was successfully established with modified paper detonators, fixed amount of explosive, and a moderated explosion distance [13]. We found that the development of brain edema and increased BBB permeability, following the early onset of bTBI, was different from cTBI. However, this alteration was suppressed by HBOT. The BBB is a highly selective permeability barrier that separates the circulating blood from the brain extracellular fluid in the central nervous system. The BBB is formed by capillary endothelial cells, which are connected by tight junctions [30]. The BBB plays an important role in protecting the neuronal microenvironment via restricting the movement of molecules from the cerebral capillaries to the brain tissue. The loss of BBB integrity may lead to cerebral hemorrhage, vasogenic edema, and neuronal cell death [31]. In this study, we evaluated the permeability of the BBB by examining the content of EB in the brain, as well as brain water content. We found that water content increased 1 h after trauma, then gradually increased at 6, 12, and 24 h, and peaked at 72 h ($p < 0.05$), but gradually decreased for up to 7 days after trauma. Meanwhile, BBB permeability was also elevated 1 h after injury in the ipsilateral hemisphere to the injury. This indicates that brain edema caused by blast injury is associated with increased BBB permeability. By contrast, both brain edema and abnormal BBB permeability were both suppressed by HBOT. This finding is also consistent with prior experimental and clinical findings that suggest HBOT can provide neuroprotection by inhibiting brain edema and BBB leakage [32–34].

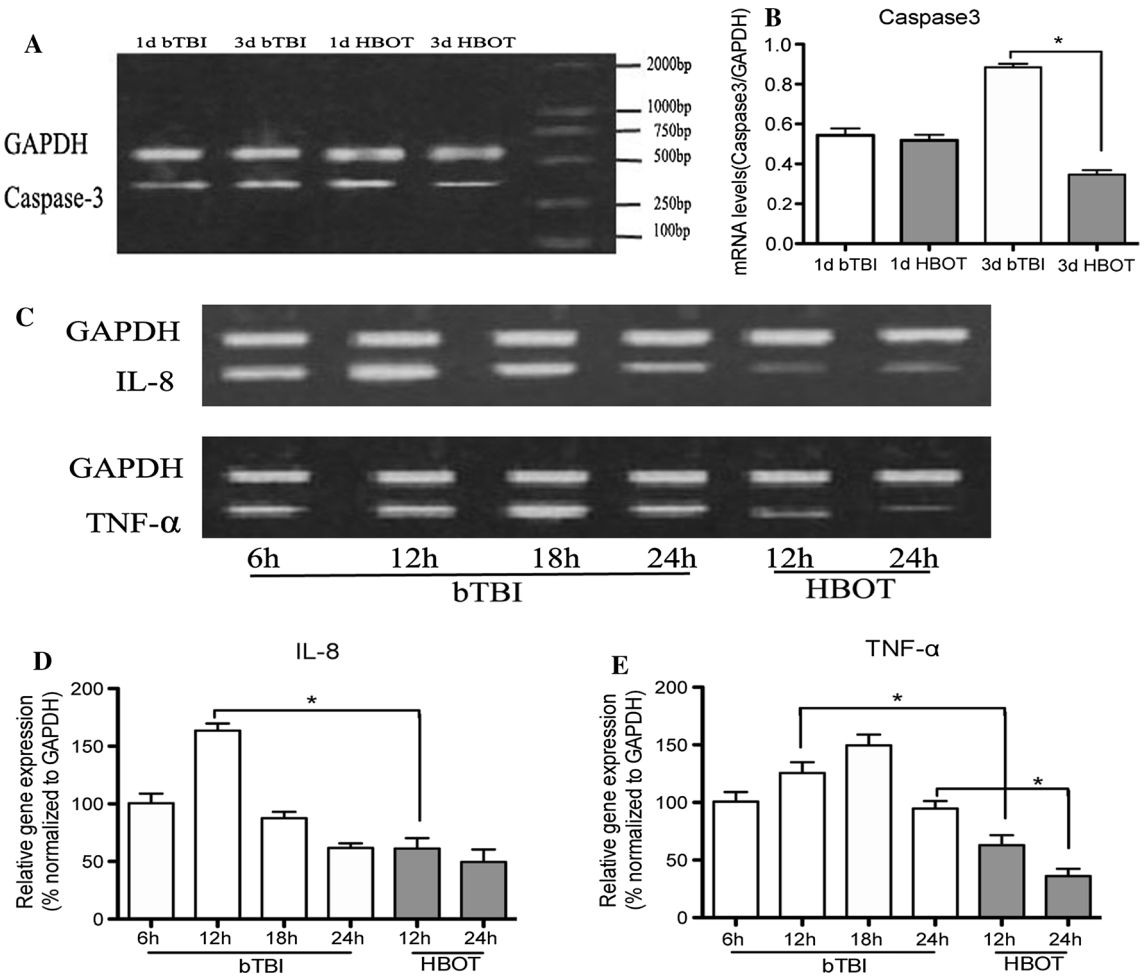

Fig. 5 HBOT inhibits the expression of caspase-3, IL-8 and TNF-α RNA after injury. **a** Representative figure of RT-PCR of caspase-3. **b** Statistical analysis of caspase-3 RNA levels in the bTBI and HBOT groups at 1 and 3 days after injury. **c** Representative figure of RT-PCR of IL-8 and TNF-α. **d** Statistical analysis of IL-8 RNA levels. The IL-8 level in the HBOT group was significantly lower compared with the level in the bTBI group at 12 h after injury. **e** Statistical analysis of TNF-α RNA levels. Compared with the bTBI group, the TNF-α level was significantly lower in the HBOT group at 12 and 24 h after injury. *Significant difference compared with the control group ($p < 0.05$); **significant difference compared with the model group ($p < 0.01$)

Previous studies have shown that MRS is a new non-invasive MRI detection technology that can be used to measure energy metabolism and biochemical changes in live tissues and organs, as well as quantitatively analyze specific compounds leading to the analysis of metabolism in local brain tissue. In brain trauma, pathophysiological changes of local brain tissue can be investigated by measuring NAA/Cr and Cho/Cr levels in brain tissue [35]. An accuracy of 81 % between NAA/Cr, Cho/Cr and lactate results detected by MRS and clinical related indicators has been reported, indicating that MRS plays important roles in evaluating the prognosis of severe craniocerebral injury [10, 11]. The characteristic component of NAA is recognized as an endogenous marker of neurons, indicating the functional status of neurons. A decrease in NAA content reflects the loss and functional damage of neurons. Choline (Cho) concentration in glial cells is significantly higher than neurons, and thus mainly indicates changes within glial cells. The increase in Cho/Cr levels represents tissue destruction, repair, or inflammatory reactions [8]. In our previous study, we found that NAA/Cr levels significantly decreased 24 h after injury, which was consistent with results published by Babikian, Cimatti and Govindaraju [35–37]. But this study found that this decrease was followed by a rebound increase 24 h after injury and a decrease again 7 days after injury. We inferred that such changes in NAA/Cr levels reflected reversible metabolic changes in neurons, which indicates that there might be neuronal damage and metabolic repression in the early stage of injury, and thus NAA/Cr levels could gradually rebound when inhibitive mechanisms slightly decreased 24 h later. However, NAA/Cr levels significantly decreased again

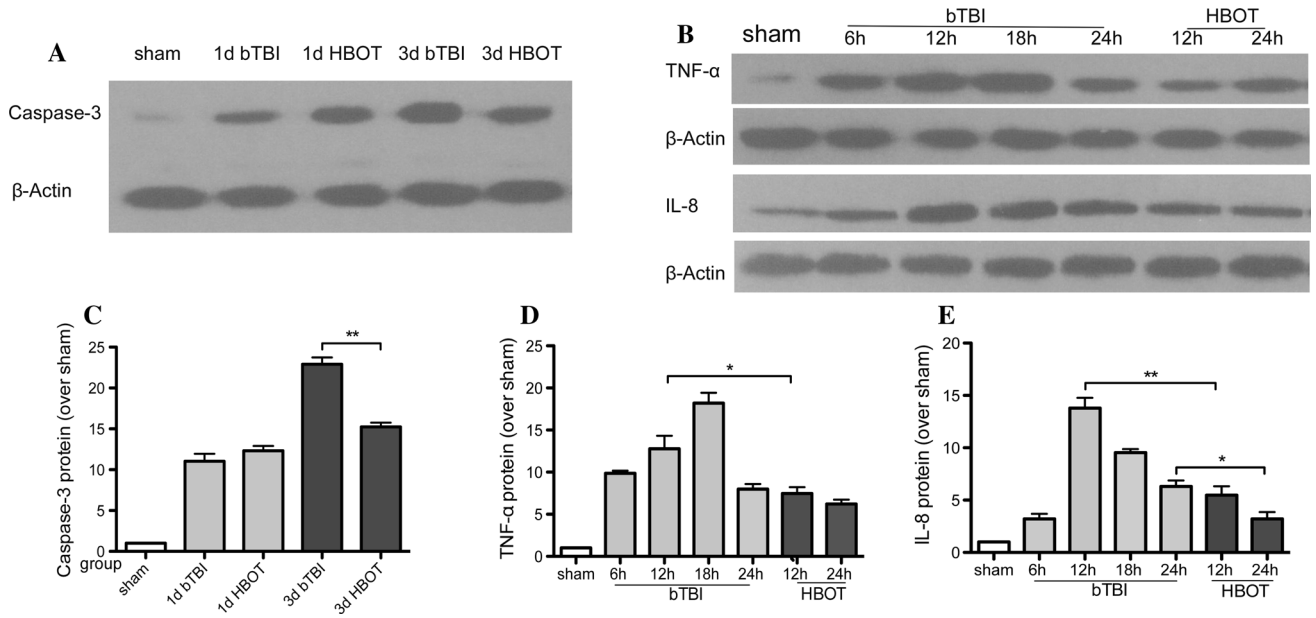

Fig. 6 HBOT reduces the protein expression of caspase-3, IL-8 and TNF-α after injury. **a** Representative western blot of caspase-3. **b** Representative western blot of IL-8 and TNF-α. **c** Statistical analysis of caspase-3 protein levels in the bTBI and HBOT groups at 1 and 3 days after injury. **d** Statistical analysis of TNF-α protein levels. Compared with the bTBI group, the TNF-α level was significantly lower in the HBOT group at 12 h after injury. **e** Statistical analysis of IL-8 protein levels. The IL-8 level in the HBOT group was significantly lower compared with the level of the bTBI group at 12 and 24 h after injury. *Significant difference compared with the control group ($p < 0.05$); **significant difference compared with the model group ($p < 0.01$)

7 days later, indicating that damaged nerve cells further degenerated via apoptosis without timely treatment. By contrast, in the HBOT group, NAA/Cr levels exhibited an advanced rebound after 12 h and then the same variation trends as the control group. But, NAA/Cr levels were higher than that of the control group after every time point, especially in the 7 days after injury. All results indicate that HBOT could elevate oxygen content in brain tissue and cerebrospinal fluid, effectively removing hypoxia in brain tissue in the early stage of brain injury. This lack of hypoxia alleviated the repression metabolism in neurons, and played important protective roles in neurons, especially in the early traumatic stage. The total amount of Cho in the bTBI group exhibited an upward trend after trauma, but slightly decreased 12–24 h later, which might have resulted from responses by injured astrocytes. One to two days after injury, neurons and glial cells in deep layers gradually exhibited swelling. This resulted in a decrease in number of cells in each voxel. Then glial cell proliferation gradually resulted in another rising trend in Cho/Cr levels. The mean Cho/Cr value in the HBOT group was significantly higher than in the control group, suggesting that HBOT could promote the repair of glial cells and functional reorganization, but the mean Cho/Cr value returned to the level of the control group 7 days later. Altogether, we believe that MRS is an effective and safe tool to research the therapeutic effect and prognosis of TBI. Also, these animal studies further confirm that HBOT, especially within 7 days of trauma, might significantly improve the prognosis of bTBI.

To further study the mechanisms underlying the therapeutic effects of HBOT on brain injury, apoptotic factors and some inflammation markers were investigated. Apoptosis, characterized morphologically by condensed nuclei, cell shrinkage, chromatin marginalization and membrane blebbing, has been suggested as an important process in bTBI [13]. Pro-apoptotic factors, including Bcl-2 and Bax, have been shown to change in explosive brain damage [38]. The caspase-3 protein is a member of the cysteine-aspartic acid protease family. Sequential activation of caspases plays a central role in the execution-phase of cell apoptosis. Our data demonstrate changes in the downstream pro-apoptotic factor caspase-3, which further supports the therapeutic effect of HBOT by decreasing cell apoptosis in explosive brain damage. Moreover, acute inflammation also plays an important role in the pathogenesis of cerebral injury and in secondary brain damage after TBI. Leukocytic infiltration, particularly by polymorphonuclear neutrophils (PMNs), is mainly characterized by its role in creating the deleterious effects of inflammation in brain injury [39–41]. Activated PMNs may induce and aggravate brain injury by recruiting many kinds of toxic mediators, including cytokines. IL-8 is a chemokine produced by macrophages and other cell types such as epithelial cells, airway smooth muscle cells and endothelial cells [42]. It is

known as neutrophil chemotactic factor, and has two primary functions. It induces chemotaxis in target cells, primarily neutrophils but also other granulocytes, causing them to migrate toward the site of infection. Following induction of IL-8 release from endothelial cells, TNF-α might be indirectly involved in PMN infiltration and associated with intervention in PMN adhesion and migration [43, 44]. In the present study, we observed that HBOT after bTBI showed an inhibitory effect on the high expression of cytokines and chemokines, including TNF-α and IL-8. These results provide evidence for a neuroprotective effect of HBOT against blast-induced inflammation in the rabbit brain.

In brief, our findings indicate that HBOT, especially within 7 days of injury onset, has a neuroprotective and therapeutic effect against bTBI injury. This may be closely associated with an inhibitory effect of HBOT on brain edema, BBB leakage, cell apoptosis, and the expression of cytokines/chemokines and neutrophil recruitment.

Acknowledgments This study was supported by research Grants from the Nature Science Youth Funding of Anhui Province (1208085QH171) and Nanjing Military Region Fund Project (10MB009). We also thank Professor Bingchang Li (Institute of Battle Surgical Research, Third Military Medicine University) for his support while creating our animal model and Daniel Smerin for his manuscript editing.

Conflict of interest We have no conflicts of interest to declare.

References

1. Huang E, Ngo M, Yee S, Held L, Norman K, Scremin AM, Scremin O (2013) Repeated blast exposure alters open field behavior recorded under low illumination. Brain Res 1529: 125–133
2. Ling G, Bandak F, Armonda R, Grant G, Ecklund J (2009) Explosive blast neurotrauma. J Neurotrauma 26:815–825
3. Davenport ND, Lim KO, Armstrong MT, Sponheim SR (2012) Diffuse and spatially variable white matter disruptions are associated with blast-related mild traumatic brain injury. Neuroimage 59:2017–2024
4. Armonda RA, Bell RS, Vo AH, Ling G, DeGraba TJ, Crandall B, Ecklund J, Campbell WW (2006) Wartime traumatic cerebral vasospasm: recent review of combat casualties. Neurosurgery 59:1215–1225; (discussion 1225)
5. Tang X, Liu KJ, Ramu J, Chen Q, Li T, Liu W (2010) Inhibition of gp91(phox) contributes towards normobaric hyperoxia afforded neuroprotection in focal cerebral ischemia. Brain Res 1348:174–180
6. Edwards ML (2010) Hyperbaric oxygen therapy. Part 1: history and principles. J Vet Emerg Crit Care 20:284–288
7. Voigt C, Forschler A, Jaeger M, Meixensberger J, Kuppers-Tiedt L, Schuhmann MU (2008) Protective effect of hyperbaric oxygen therapy on experimental brain contusions. Acta Neurochir Suppl 102:441–445
8. Palzur E, Zaaroor M, Vlodavsky E, Milman F, Soustiel JF (2008) Neuroprotective effect of hyperbaric oxygen therapy in brain injury is mediated by preservation of mitochondrial membrane properties. Brain Res 1221:126–133
9. Rockswold SB, Rockswold GL, Defillo A (2007) Hyperbaric oxygen in traumatic brain injury. Neurol Res 29:162–172
10. Qian J, Qian B, Lei H (2013) Reversible loss of N-acetylaspartate after 15-min transient middle cerebral artery occlusion in rat: a longitudinal study with in vivo proton magnetic resonance spectroscopy. Neurochem Res 38:208–217
11. Sidaros A, Herning M (2007) Magnetic resonance imaging in severe traumatic brain injury. Ugeskr Laeg 169:214–216
12. Kamnaksh A, Kovesdi E, Kwon SK, Wingo D, Ahmed F, Grunberg NE, Long J, Agoston DV (2011) Factors affecting blast traumatic brain injury. J Neurotrauma 28:2145–2153
13. Yong-Ming Z, Jia-Chuan L, Yan-Yan Y, Wen-Jiang S, Hong T, Bing-Cang L, Liang-Chao Z (2012) Effective protection of rabbits' explosive brain injury through blocking gap junction communication. Afr Health Sci 12:552–556
14. Soares DP, Law M (2009) Magnetic resonance spectroscopy of the brain: review of metabolites and clinical applications. Clin Radiol 64:12–21
15. Li CX, Wang Y, Gao H, Pan WJ, Xiang Y, Huang M, Lei H (2008) Cerebral metabolic changes in a depression-like rat model of chronic forced swimming studied by ex vivo high resolution 1H magnetic resonance spectroscopy. Neurochem Res 33: 2342–2349
16. Brugger S, Davis JM, Leucht S, Stone JM (2011) Proton magnetic resonance spectroscopy and illness stage in schizophrenia—a systematic review and meta-analysis. Biol Psychiatry 69: 495–503
17. Ren C, Gao X, Niu G, Yan Z, Chen X, Zhao H (2008) Delayed postconditioning protects against focal ischemic brain injury in rats. PLoS One 3:e3851
18. Yang DY, Pan HC, Chen CJ, Cheng FC, Wang YC (2007) Effects of tissue plasminogen activator on cerebral microvessels of rats during focal cerebral ischemia and reperfusion. Neurol Res 29:274–282
19. Magnuson J, Leonessa F, Ling GS (2012) Neuropathology of explosive blast traumatic brain injury. Curr Neurol Neurosci Rep 12:570–579
20. Dewall J (2010) The ABCs of TBI. Evidence-based guidelines for adult traumatic brain injury care. J Emerg Med Serv 35:54-61; quiz 63
21. Ling GS, Ecklund JM (2011) Traumatic brain injury in modern war. Curr Opin Anaesthesiol 24:124–130
22. Liu Z, Jiao QF, You C, Che YJ, Su FZ (2006) Effect of hyperbaric oxygen on cytochrome C, Bcl-2 and Bax expression after experimental traumatic brain injury in rats. Chin J Traumatol 9:168–174
23. Niklas A, Brock D, Schober R, Schulz A, Schneider D (2004) Continuous measurements of cerebral tissue oxygen pressure during hyperbaric oxygenation–HBO effects on brain edema and necrosis after severe brain trauma in rabbits. J Neurol Sci 219:77–82
24. Wright JK, Zant E, Groom K, Schlegel RE, Gilliland K (2009) Case report: treatment of mild traumatic brain injury with hyperbaric oxygen. Undersea Hyperb Med 36:391–399
25. Rockswold SB, Rockswold GL, Zaun DA, Zhang X, Cerra CE, Bergman TA, Liu J (2010) A prospective, randomized clinical trial to compare the effect of hyperbaric to normobaric hyperoxia on cerebral metabolism, intracranial pressure, and oxygen toxicity in severe traumatic brain injury. J Neurosurg 112: 1080–1094
26. Edwards ML (2010) Hyperbaric oxygen therapy. Part 2: application in disease. J Vet Emerg Crit Care 20:289–297
27. Harch PG, Kriedt C, Van Meter KW, Sutherland RJ (2007) Hyperbaric oxygen therapy improves spatial learning and memory in a rat model of chronic traumatic brain injury. Brain Res 1174:120–129

28. Wang GH, Zhang XG, Jiang ZL, Li X, Peng LL, Li YC, Wang Y (2010) Neuroprotective effects of hyperbaric oxygen treatment on traumatic brain injury in the rat. J Neurotrauma 27:1733–1743
29. Marx RE, Ehler WJ, Tayapongsak P, Pierce LW (1990) Relationship of oxygen dose to angiogenesis induction in irradiated tissue. Am J Surg 160:519–524
30. Ballabh P, Braun A, Nedergaard M (2004) The blood–brain barrier: an overview: structure, regulation, and clinical implications. Neurobiol Dis 16:1–13
31. Lee JH, Cui HS, Shin SK, Kim JM, Kim SY, Lee JE, Koo BN (2013) Effect of propofol post-treatment on blood–brain barrier integrity and cerebral edema after transient cerebral ischemia in rats. Neurochem Res 38:2276–2286
32. Rosenthal RE, Silbergleit R, Hof PR, Haywood Y, Fiskum G (2003) Hyperbaric oxygen reduces neuronal death and improves neurological outcome after canine cardiac arrest. Stroke 34: 1311–1316
33. Hollin SA, Sukoff MH, Jacobson JH 2nd (1968) The protective effect of hyperbaric oxygenation in experimentally produced cerebral edema and compression. Prog Brain Res 30:479–489
34. Gill AL, Bell CN (2004) Hyperbaric oxygen: its uses, mechanisms of action and outcomes. QJM 97:385–395
35. Marino S, Zei E, Battaglini M, Vittori C, Buscalferri A, Bramanti P, Federico A, De Stefano N (2007) Acute metabolic brain changes following traumatic brain injury and their relevance to clinical severity and outcome. J Neurol Neurosurg Psychiatry 78:501–507
36. McLean MA, Cross JJ (2009) Magnetic resonance spectroscopy: principles and applications in neurosurgery. Br J Neurosurg 23:5–13
37. Lin JW, Tsai JT, Lee LM, Lin CM, Hung CC, Hung KS, Chen WY, Wei L, Ko CP, Su YK, Chiu WT (2008) Effect of hyperbaric oxygen on patients with traumatic brain injury. Acta Neurochir Suppl 101:145–149
38. Wennersten A, Holmin S, Mathiesen T (2003) Characterization of Bax and Bcl-2 in apoptosis after experimental traumatic brain injury in the rat. Acta Neuropathol 105:281–288
39. Kang GH, Yan BC, Cho GS, Kim WK, Lee CH, Cho JH, Kim M, Kang IJ, Won MH, Lee JC (2012) Neuroprotective effect of fucoidin on lipopolysaccharide accelerated cerebral ischemic injury through inhibition of cytokine expression and neutrophil infiltration. J Neurol Sci 318:25–30
40. Chamorro A, Hallenbeck J (2006) The harms and benefits of inflammatory and immune responses in vascular disease. Stroke 37:291–293
41. Samson Y, Lapergue B, Hosseini H (2005) Inflammation and ischaemic stroke: current status and future perspectives. Revue Neurol 161:1177–1182
42. Hedges JC, Singer CA, Gerthoffer WT (2000) Mitogen-activated protein kinases regulate cytokine gene expression in human airway myocytes. Am J Respir Cell Mol Biol 23:86–94
43. Emerich DF, Dean RL 3rd, Bartus RT (2002) The role of leukocytes following cerebral ischemia: pathogenic variable or bystander reaction to emerging infarct? Exp Neurol 173:168–181
44. Witko-Sarsat V, Rieu P, Descamps-Latscha B, Lesavre P, Halbwachs-Mecarelli L (2000) Neutrophils: molecules, functions and pathophysiological aspects. Lab Invest 80:617–653